Spin-Orbit Coupling in the Proton-Proton Interaction*

J. L. GAMMEL AND R. M. THALER
Los Alamos Scientific Laboratory, University of California, Los Alamos, New Mexico
(Received March 20, 1957)

The proton-proton interaction is examined at high energies. A phenomenological potential is derived from the scattering data. In the triplet state, this potential has a strong short-range ($\sim 0.4\times10^{-13}$ cm) repulsive core region, outside of which a long-ranged tensor force and extremely short-range spin-orbit ($\mathbf{L}\cdot\mathbf{S}$) force are effective. Good fits can be obtained to all the p-p data below 310 Mev. More important, at 310 Mev the calculated phase shifts are very close to the phase shifts which give the best fit found in a phase-shift analysis of the 310-Mev data, and at all lower energies precision fits to the experimental data can be obtained by very slight (if any) changes in the calculated phase shifts.

I. INTRODUCTION

A PREVIOUS attempt to fit the two-nucleon data by means of central and tensor potentials,[1] while successful in many respects, failed to reproduce the proton-proton polarization data at 170 and 310 Mev. A phase-shift analysis[2] of the 310-Mev p-p scattering data shows that the reason for this failure is that the triplet p-wave phase shifts are split in a manner inconsistent with the tensor force. Some additional force which splits the triplet P phase shifts differently than the tensor force is necessary. The spin-orbit ($\mathbf{L}\cdot\mathbf{S}$) force is such a force.

For this reason the potentials discussed in this work are assumed to be of the form:

$$V(r)=V_C(r)+V_T(r)S_{12}+V_{LS}(r)\mathbf{L}\cdot\mathbf{S}, \quad (1)$$

where the subscripts C, T, and LS stand for central, tensor, and spin-orbit, respectively, and where S_{12} is the tensor operator,[3] $\mathbf{L}\cdot\mathbf{S}$ is the spin-orbit operator with eigenvalues

$$\mathbf{L}\cdot\mathbf{S}=\tfrac{1}{2}[J(J+1)-L(L+1)-S(S+1)]. \quad (2)$$

It is also assumed that $V_C(r)$, $V_T(r)$, and $V_{LS}(r)$ have a general spin and parity dependence, but are energy-independent.

It will be shown below that a potential of the form of Eq. (1) can reproduce all the proton-proton data below 310 Mev to good accuracy. More important, the phase shifts calculated from this potential are very close to the phase shifts of solution 1 of Stapp *et al.* at 310 Mev, and at all lower energies precision fits to the experimental data can be obtained by very slight (if any) changes in the calculated phase shifts.

II. 310-MEV PROTON-PROTON SINGLET PHASE SHIFTS

Examination of the phase shifts resulting from the phase shift analysis[2] of the Berkeley p-p data at 310 Mev immediately discloses the possibility of understanding the singlet even-parity part of the nucleon-nucleon interaction in terms of a simple potential (a repulsive core with a monotonic attractive potential outside). Three solutions (1, 3, and 6) of the five best solutions (1, 4, and 6) found by Stapp *et al.* have singlet even-parity phase shifts which are close to singlet even-parity phase shifts calculated from potentials which fit the singlet scattering length and effective range.[1] These potentials were taken to be of the form

$$^1V^+(r)=\begin{cases}+\infty, & r<{}^1r_0^+\\ -{}^1V_C^+\exp(-{}^1\mu_C^+\,r)/{}^1\mu_C^+\,r, & r>{}^1r_0^+.\end{cases} \quad (3)$$

The singlet even-parity potential which fits the low-energy data and which also yields phase shifts at 310 Mev which are close to those of solutions 1 and 3 of Stapp *et al.* is described by Eq. (3) with

$$^1r_0^+=0.4, \quad ^1\mu_C^+=1.45, \quad ^1V_C^+=425.5 \text{ Mev}, \quad (4)$$

where here and throughout the paper we specify r in units of 10^{-13} cm and μ in units of 10^{13} cm^{-1}.

The potential of reference 1 with $^1r_0=0.3$, $^1\mu_C^+=1.26$, and $^1V_C^+=227.4$ Mev yields phase shifts at 310 Mev which are close to the singlet even-parity phase shifts of Stapp's solution 6. However, it is possible to eliminate solution 6 on other grounds.[4] The remaining two solutions (2 and 4) have singlet phase shifts which cannot be understood in terms of a simple potential which fits the low-energy data. Solutions 2 and 4 are

* Work performed under the auspices of the U. S. Atomic Energy Commission.

[1] Gammel, Christian, and Thaler, Phys. Rev. **175**, 311 (1957).

[2] Stapp, Ypsilantis, and Metropolis, Phys. Rev. **105**, 302 (1957).

[3] J. Ashkin and T.-Y. Wu, Phys. Rev. **73**, 986 (1948).

[4] H. A. Bethe (private communication). Professor Bethe observes that "the phase shifts of solution 6 give a very small result for the coefficient C in the notation of Wolfenstein as used in the paper by Chamberlain, Segrè, Tripp, Wigand, and Ypsilantis [Phys. Rev. **105**, 288 (1957)]. C determines the polarization obtainable in scattering from a complex nucleus. This polarization is known to be large. The phase shifts of Stapp *et al.* give only the contribution of $T=1$ states to C. Solutions 1–4 give about 60% of the total value of C required. The remaining 40% has to come from $T=0$ scattering which seems reasonable. The phase shifts of solution 6 give less than 20% of the required C from $T=1$ states, which seems unreasonable."

The authors believe that the phase shifts of solution 6 would be very difficult to fit with a potential. Moreover, such a potential would have to be in qualitative disagreement with what we would expect from meson theory.

TABLE I. A comparison of the 310-Mev triplet even-parity phase shifts as calculated from the potential of Eqs. (3) and (4) and as obtained from the phase-shift analysis of Stapp *et al.*, solutions 1 and 3. The entries are twice the nuclear Blatt-Biedenharn shifts in radians.

	Calculated from potential	Solution 1	Solution 3
$\delta(^1S_0)$	−0.3280	−0.3526	−0.3822
$\delta(^1D_2)$	0.5328	0.4485	0.4643
$\delta(^1G_4)$	0.0893	0.0349	0.038

therefore not considered in this paper. The singlet phase shifts for solutions 1 and 3 of Stapp *et al.* are compared with the singlet phase shifts calculated from the potential of Eqs. (3) and (4) in Table I.

The fact that it is possible, then, to fit the singlet scattering length and effective range and the 310-Mev singlet even-parity phase shifts by the same potential leads to a basic assumption of the present work, *viz.*, that the singlet even-parity interaction is given by Eqs. (3) and (4) for $E \lesssim 310$ Mev.

The $^1D_2$ phase shift calculated from the potential of Eqs. (3) and (4) is considerably larger than postulated by many other workers.[5] It will be shown below (Sec. III) that such small or negative $^1D_2$ phase shifts are inconsistent with the description of the singlet even parity interaction in terms of a potential, and that this conclusion is not at all influenced by the potential shape which has been chosen in the present work.

III. $^1D_2$ PHASE SHIFT

For all of the five best solutions of Stapp *et al.*, the $^1S_0$ phase shift is negative and the $^1D_2$ phase shift is positive at 310 Mev. Since the interaction in the $^1S_0$ state is attractive at low energies, it is difficult to avoid the picture of a potential which has a repulsive core and is attractive outside. One way to produce a small $^1D_2$ phase shift at 310 Mev might be to use a potential which is repulsive at short distances, attractive at intermediate distances, and repulsive again at large distances. At 310 Mev the impact parameter for D waves is about 1.1. Thus, the outermost repulsive part of the potential would have to extend beyond 1.1. Otherwise, it is clearly possible to produce a larger rather than a smaller $^1D_2$ phase shift at 310 Mev than that calculated from a simpler potential. This follows from the fact that addition of a repulsive tail requires compensation by an increase in the depth of the attractive region in order to fit the low-energy data (the size of the innermost repulsive region must be maintained to give negative $^1S_0$ phase shifts at 310 Mev). The increase in depth may increase rather than decrease the $^1D_2$ phase shift at 310 Mev, if the attractive region extends beyond 1.1.

[5] See *Proceedings of the Sixth Annual Rochester Conference on High-Energy Physics* (Interscience Publishers, Inc., New York, 1956), Session II.

The effective range ρ is given by[6]

$$\rho = 2\int_0^\infty \left[\left(\frac{r}{a}-1\right)^2 - u^2\right]dr, \tag{5}$$

where a is the singlet scattering length. Since the singlet scattering length is large, this is approximately

$$\rho \approx 2\int_0^\infty (1-u^2)dr = 2r_0 + 2\int_{r_0}^\infty (1-u^2)dr, \tag{6}$$

where r_0 is the radius of the hard core. Since $u(r_0)=0$ and $u(\infty)=1$, the contribution to the effective range from the attractive region cannot exceed $\frac{4}{3}s$, where s is the size of the attractive region. Thus

$$\rho < 2r_0 + \tfrac{4}{3}s, \tag{6.1}$$

or

$$s > \tfrac{3}{4}[\rho - 2r_0]. \tag{6.2}$$

Since $\rho = 2.7$ and $^1r_0^+ \approx 0.4$, this gives $s \gtrsim 1.4$, so that the attractive region must extend to at least $r \approx 1.8$, even if there is no repulsive tail. The inclusion of a repulsive tail implied that the attractive region must extend beyond $r \approx 1.8$. However, for D-waves the impact parameter is less than 1.8 for energies greater than 130 Mev, so that it is clear that at high energies the addition of a repulsive tail tends to increase rather than decrease the $^1D_2$ phase shift.

This conclusion is in agreement with the results of reference 1. Table II, reference 1, shows that as the core size increases the attractive potential is drawn in towards the core edge ($^1\mu_c^+$ increases). The $^1D_2$ phase shifts at 310 Mev for various core sizes are shown in Table II. The $^1D_2$ phase shift increases rather than decreases as the potential is drawn in.

An extreme model is an attractive potential drawn right against the core edge (sticky hard core). For such a model one may use an energy and angular momentum boundary condition that the derivative of the wave

TABLE II. The $^1S_0$ and $^1D_2$ phase shifts calculated from various potentials and compared with the $^1S_0$ and $^1D_2$ phase shifts of Stapp *et al.*

$^1r_0^+$ (10^{-13} cm)	$^1V_c^+$ (Mev)	$^1\mu_c^+$ (10^{13} cm^{-1})	$^1S_0$	$^1D_2$
0.1	77.24	0.97	0.712	0.305
0.2	128.8	1.1	0.343	0.366
0.3	227.4	1.26	0.000	0.441
0.4	425.5	1.45	−0.328	0.533
0.5	896.6	1.70	−0.632	0.639
0.6	2078	2.00	−0.924	0.755
0.8	23 207	3.00	−1.424	0.976
Solution 1 of Stapp *et al.*			−0.353	0.449
Solution 3			−0.382	0.464
Solution 2			−0.681	0.152
Solution 4			−0.941	0.169
Solution 6			+0.009	0.483

[6] H. A. Bethe, Phys. Rev. **76**, 38 (1949), Eq. (14) and accompanying discussion.

function vanish at the edge of the core. This boundary condition makes the singlet scattering length infinite. The singlet effective range and the 310-Mev $^1S_0$ phase shift for solution 1 of Stapp *et al.* cannot be fitted simultaneously with such a model. If we choose not to fit the effective range, the core size determined by fitting the 310-Mev $^1S_0$ phase shift is about $(\pi/4)$. (For this core size the effective range is about 1.6 instead of 2.7.) It is now easy to calculate the $^1D_2$ phase shift as a function energy. At 310 Mev, $\delta(^1D_2)$ $\sim 14.5°$, which is close to the least $^1D_2$ phase shift shown in Table II.

As long as it is assumed that the interaction is the same in the $^1S_0$ and $^1D_2$ states, it appears that the 310-Mev $^1D_2$ phase shift is largely determined by the singlet scattering length, effective range, and 310-Mev $^1S_0$ phase shift, and must be about 15° regardless of the shape of the potential.

Only solutions 1, 3, and 6 of Stapp *et al.* satisfy this condition. As previously noted, solution 6 is ruled out on other grounds.[4] Moreover, there appears to be no reason at present not to adopt the more detailed potential given in Eqs. (3) and (4).

The problem of determining a shape for the singlet even-parity interaction which fits the singlet scattering length, effective range, and the singlet phase shifts for Solution 1 of Stapp *et al.* more precisely should be investigated. It seems adequate at present, however, simply to characterize the potential by a core size, and a depth and range for some given shape of the attractive part. In this work the Yukawa shape is chosen.

IV. EVIDENCE ABOUT THE SPIN-ORBIT FORCE FROM THE 310-MEV DATA

From the order of the triplet P phase shifts for either solutions 1 or 3 of Stapp *et al.*, it is evident that both a spin-orbit and a tensor term must be present in the triplet odd-parity interaction.[7]

In order to fit either solution 1 or 3, the spin orbit term must be attractive in the $^3P_2$ state and repulsive in the $^3P_0$ and $^3P_1$ states. As is shown now, this follows from the order of the triplet P phase shifts, $\delta(^3P_2) > \delta(^3P_0) > \delta(^3P_1)$.

For any potential let

$$V = -\frac{m}{\hbar^2}\frac{1}{4\pi}\int dr V(r) j_1^2(kr), \tag{7}$$

where $V(r)$ represents the radial part of the central, tensor, or spin-orbit potential. Then in Born approximation,[8-10] the phase shifts are

$$\delta(^3P_0) = V_C - 4V_T - 2V_{LS}, \tag{8.1}$$

$$\delta(^3P_1) = V_C + 2V_T - V_{LS}, \tag{8.2}$$

$$\delta(^3P_2) = V_C - \tfrac{2}{5}V_T + V_{LS}, \tag{8.3}$$

Table III. Order of the P-wave phase shifts for various signs of the tensor and spin-orbit forces.

Tensor	Spin-orbit	Comment
Attractive in $^3P_0$	Attractive in $^3P_0$	$\delta(^3P_0) > \delta(^3P_2)$
Repulsive in $^3P_0$	Repulsive in $^3P_0$	$\delta(^3P_0) < \delta(^3P_1)$
Repulsive in $^3P_0$	Attractive in $^3P_0$	$\delta(^3P_1) > \delta(^3P_2)$
Attractive in $^3P_0$	Repulsive in $^3P_0$	Allowed

where the subscripts C, T, and LS stand for the central, tensor, and spin-orbit potentials, respectively. The various possibilities are shown in Table III. Thus the signs of the tensor and spin-orbit forces are fixed by qualitative arguments. This argument, however, favors solution 1 of Stapp *et al.*, since solution 3 has the wrong sign for the $J=2$ coupling constant when the tensor force has the sign determined above.

The order of the F-wave phase shifts of solution 1 is such that no spin-orbit force is short-ranged, of a range such that it is important for P waves but not for F waves.

V. EVIDENCE ABOUT THE SPIN-ORBIT FORCE FROM LOW ENERGIES

A phase-shift analysis of the 18.3-Mev p-p data for the triplet P phase shifts based on the assumption that the singlet even-parity phase shifts are given by the potential Eq. (4) results in two solutions; for both of these solutions the order of the triplet P phase shifts is that expected from a tensor force.[11]

Since no spin-orbit force is required at low energies, it may be concluded again that the spin-orbit force is short-ranged.

There is evidence from the position of the minimum for 90-Mev n-p scattering that the order of the triplet P phase shifts is more nearly that expected from a tensor force rather than a spin-orbit force. However, this conclusion is based on experience gained in making detailed calculations, and it is difficult to make even a convincing qualitative argument for it.

Some evidence for both these points is found in the results of Feshbach and Lomon.[12] The order of their

[7] See Sec. V of reference 2.

[8] Of course, the $^3P_2$ state is coupled to the $^3F_2$ state, and it matters exactly what parametrization of the S matrix is meant, $\delta(^3P_2)$ is what Stapp calls the nuclear bar phase shift. It is perhaps a little more accurate to think of $\delta(^3P_2)$ as the element x_1 of the tangent matrix; see Eq. (A.10) of Stapp *et al.* For small x_1, $\delta(^3P_2) = x_1$ according to Eq. (A.12) of Stapp *et al.*

[9] Born's approximation suffices for this discussion. Presumably there are no bound triplet P states, and from the n-p total cross section data it appears that none of the triplet P phase shifts passes through 90° at any energy. We are only going to draw qualitative conclusions from Born's approximation, which is qualitatively valid under these conditions.

[10] The factors in front of V_T and V_{LS} come from Eq. (2) and the expressions for the diagonal elements of S_{12}, the tensor operator, given in reference 3.

[11] J. L. Gammel and R. M. Thaler (unpublished). For one solution the tensor force would have to be attractive in the $^3P_0$ state, for the other the tensor force would have to be repulsive in the $^3P_0$ state. We have already concluded that the tensor force is attractive in the $^3P_0$ state and so could have fit the phase shifts. However, we chose to fit the angular distribution directly.

[12] H. Feshbach and F. Lomon, Phys. Rev. **102**, 891 (1956).

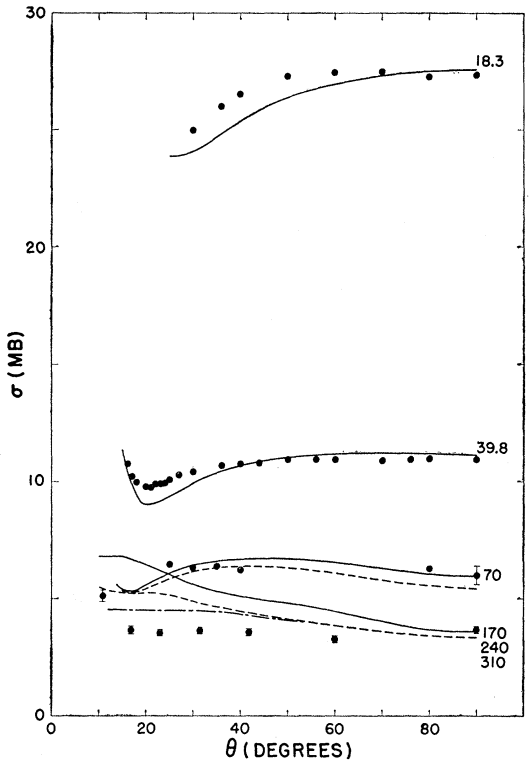

FIG. 1. The proton-proton differential cross section for several different energies. The solid curves represent the fits to the data with the Yukawa-shaped tensor force. The dashed curves represent the fit with the tensor force given by Eqs. (11) and (12). Where no dashed curve appears, the dashed and solid curves are nearly identical. The differential cross sections calculated from a given potential are practically indistinguishable for 170, 240, and 310 Mev. The calculated curves shown are for 310 Mev. The data points shown are for 170 Mev. The 310-Mev experimental differential cross section is 3.7 mb independent of angle for angles greater than 10°. The alternately long- and short-dashed curve shows the result of using the singlet phase shifts of solution 1 of Stapp *et al.* together with the triplet phase shifts calculated from the triplet potential of Eqs. (11) and (12).

triplet P phase shifts cannot be explained by a tensor force so weak as not to produce ^3P bound states or resonances. They failed to get the correct sign for the Coulomb interference in p-p scattering at low energies,[13] and the position of the minimum for 90-Mev n-p scattering is incorrect.

VI. DETAILED CALCULATION

The arguments presented in the two preceding sections suggest that a potential which fits the low-energy scattering data and the phase shifts of solution 1 of Stapp *et al.* should have the following qualitative features: (1) The tensor force is long-ranged and attractive in the $^3P_0$ state. (2) The spin-orbit force is short-ranged and repulsive in the $^3P_0$ state.

We have assumed that the form of the triplet

[13] A. G. Saperstein and L. Durand, III, Phys. Rev. **104**, 1102 (1956).

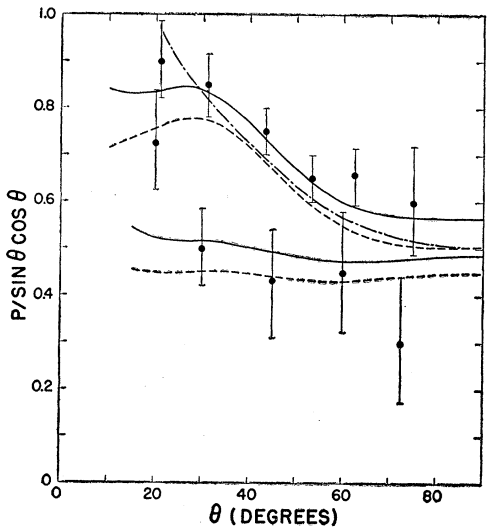

FIG. 2. The polarization at 170 and 310 Mev. The lower set of curves and data points are for 170 Mev, the upper set for 310 Mev. The curves are coded as in Fig. 1.

odd-parity potential is

$$\begin{aligned} V &= +\infty, && r<r_0 \\ &= -[S_{12}V_T(r)+\mathbf{L}\cdot\mathbf{S}V_{LS}(r)], && r>r_0 \end{aligned} \tag{9}$$

where $V_T(r)$ and $V_{LS}(r)$ have the form

$$V(r)=V\exp(-\mu r)/\mu r. \tag{9.1}$$

No long-range central force (the hard core is a short-range central force, of course) is used in fitting the data. Only slight improvement of the fit can be obtained with the addition of a long-range central potential, and for these slightly improved fits the central force is very weak and repulsive. We have thought it best to omit the triplet odd central potential entirely.

We first adjust the core size, and the ranges and depths of the tensor and spin-orbit potentials to fit the triplet P and F phase shifts and the $^3P_2+^3F_2$ coupling constant for solution 1 of Stapp *et al.* As expected, the spin-orbit force was found to have a very small range (<0.3). Consequently, only the tensor force plays a role at low energy.

We found, however, that the 90° differential cross sections calculated at 18.3 and 70 Mev were too small; it was necessary to increase the depth of the tensor force to fit these low-energy data.

The core size and spin-orbit force were then held fixed at the values determined from the fit to the 310-Mev phase shifts, and the range and depth of the tensor force were readjusted to reproduce the 90° differential cross section at 18.3 and 70 Mev. The deeper and shorter-ranged tensor force so determined was then used at 310 Mev and the core size and spin-orbit range and depth readjusted to fit the triplet phase shifts. Although the fit to the 310-Mev phase shifts was necessarily worsened, the resulting potentials provide

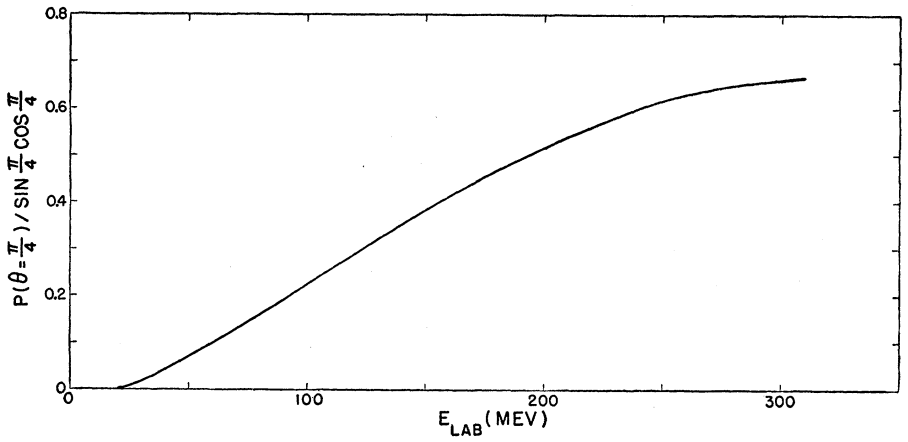

FIG. 3. The polarization at 45° as a function of energy as calculated from the potentials of Eqs. (9), (11), and (12).

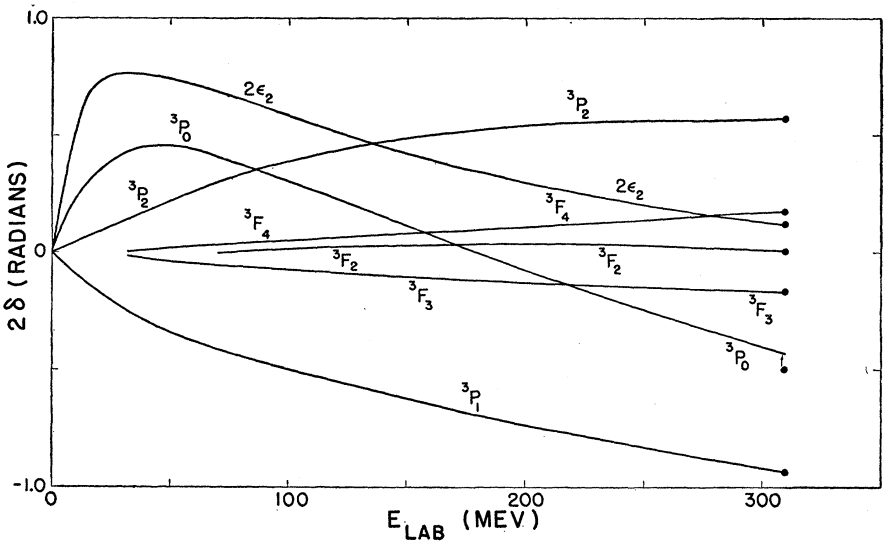

FIG. 4. The triplet phase shifts calculated from the potentials of Eqs. (9), (11), and (12). The dots at 310 Mev are the phase shifts for solution 1 of Stapp *et al.*

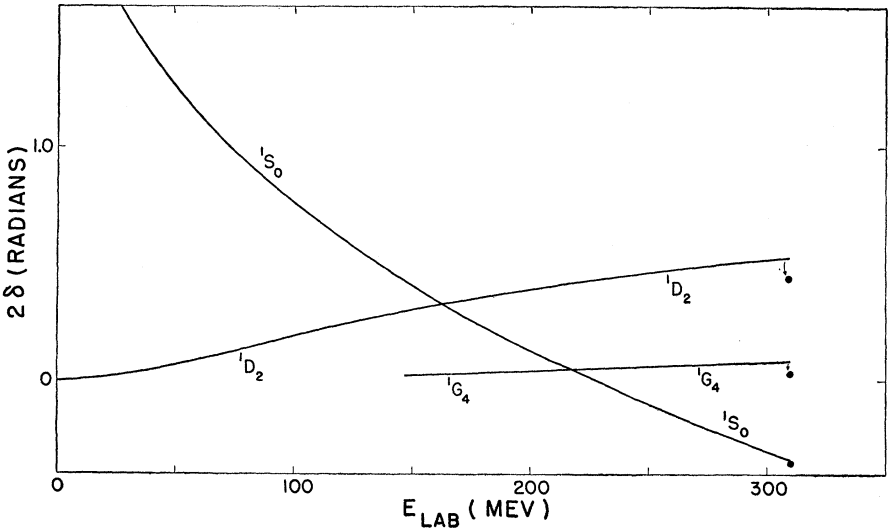

FIG. 5. The singlet phase shifts calculated from the potential of Eqs. (3) and (4). The dots at 310 Mev are the phase shifts for solution 1 of Stapp *et al.*

TABLE IV Singlet and triplet phase shifts *versus* energy. The tabular entries are twice the nuclear Blatt-Biedenharn phase shifts in radians.

(a) Singlet phase shifts calculated from the potential of Eqs. (3) and (4).

E (Mev)	$^1S_0$	$^1D_2$	$^1G_4$	E (Mev)	$^1S_0$	$^1D_2$	$^1G_4$
10	1.896	0.003	0.000	160	0.351	0.325	0.031
20	1.717	0.013	0.000	180	0.240	0.362	0.037
30	1.542	0.028	0.000	200	0.134	0.393	0.427
40	1.390	0.048	0.001	220	0.039	0.427	0.054
60	1.136	0.094	0.003	240	−0.049	0.455	0.061
80	0.932	0.145	0.006	260	−0.137	0.477	0.066
100	0.757	0.192	0.011	280	−0.219	0.502	0.077
120	0.608	0.241	0.017	300	−0.292	0.525	0.087
140	0.471	0.283	0.022	320	−0.365	0.539	0.091

(b) Triplet phase shifts calculated from the Yukawa-shaped triplet odd-parity potential given by Eqs. (9), (9.1), and (10).

E (Mev)	$^3P_0$	$^3P_1$	$^3F_2$	$^3H_5$	$^3H_6$	$^3P_2$	$^3F_2$	$2\epsilon(2)$	$^3F_4$	$^3H_4$	$2\epsilon(4)$
10	0.195	−0.088	−0.001	0.000	0.000	0.038	−0.002	0.551	0.000	0.000	0.625
20	0.354	−0.174	−0.006	0.000	0.000	0.093	−0.006	0.678	0.003	0.000	1.026
30	0.438	−0.242	−0.013	−0.001	−0.000	0.048	−0.008	0.710	0.007	−0.002	1.030
40	0.473	−0.298	−0.022	−0.002	0.000	0.199	−0.008	0.705	0.012	−0.003	1.141
60	0.473	−0.388	−0.039	−0.005	0.002	0.291	−0.002	0.663	0.025	−0.006	1.165
80	0.426	−0.462	−0.056	−0.009	0.004	0.367	−0.005	0.605	0.037	−0.009	1.226
100	0.365	−0.525	−0.070	−0.014	0.005	0.433	0.015	0.545	0.051	−0.011	1.196
120	0.294	−0.584	−0.085	−0.019	0.007	0.485	0.021	0.490	0.062	−0.013	1.210
140	0.225	−0.637	−0.095	−0.022	0.010	0.531	0.029	0.439	0.076	−0.011	1.178
160	0.153	−0.684	−0.107	−0.029	0.009	0.565	0.032	0.393	0.086	−0.013	1.141
180	0.081	−0.734	−0.119	−0.031	0.013	0.593	0.033	0.354	0.099	−0.011	1.125
200	0.017	−0.776	−0.125	−0.034	0.015	0.618	0.037	0.317	0.113	−0.008	1.064
220	−0.051	−0.818	−0.136	−0.042	0.013	0.631	0.032	0.284	0.122	−0.009	1.014
240	−0.117	−0.862	−0.147	−0.044	0.017	0.642	0.029	0.256	0.135	−0.005	0.980
260	−0.176	−0.900	−0.151	−0.045	0.021	0.653	0.028	0.229	0.152	0.000	0.916
280	−0.234	−0.934	−0.160	−0.052	0.018	0.653	0.021	0.204	0.165	0.000	0.850
300	−0.296	−0.974	−0.171	−0.057	0.018	0.649	0.010	0.183	0.177	0.000	0.804
320	−0.353	−1.010	−0.177	−0.056	0.024	0.649	0.004	0.163	0.196	0.006	0.752

(c) Triplet phase shifts calculated from the triplet odd-parity potential given by Eqs. (9), (11), and (12).

E (Mev)	$^3P_0$	$^3P_1$	$^3F_3$	$^3H_5$	$^3H_6$	$^3P_2$	$^3F_2$	$2\epsilon(2)$	$^3F_4$	$^3H_4$	$2\epsilon(4)$
10	0.199	−0.091	−0.001	0.000	0.000	0.038	−0.002	0.593	0.000	0.000	0.641
20	0.353	−0.176	−0.007	0.000	0.000	0.091	−0.007	0.730	0.003	0.000	1.013
30	0.426	−0.242	−0.014	−0.001	0.000	0.143	−0.009	0.766	0.008	−0.002	1.044
40	0.452	−0.295	−0.024	−0.002	0.000	0.189	−0.010	0.762	0.013	−0.003	1.148
60	0.435	−0.378	−0.041	−0.006	0.002	0.271	−0.003	0.716	0.027	−0.007	1.179
80	0.376	−0.446	−0.059	−0.010	0.004	0.335	0.005	0.651	0.040	−0.010	1.239
100	0.306	−0.502	−0.072	−0.015	0.006	0.391	0.017	0.581	0.053	−0.011	1.214
120	0.229	−0.555	−0.087	−0.020	0.007	0.433	0.024	0.515	0.064	−0.013	1.229
140	0.154	−0.603	−0.097	−0.024	0.011	0.472	0.033	0.454	0.078	−0.012	1.200
160	0.078	−0.646	−0.108	−0.031	0.009	0.501	0.036	0.398	0.087	−0.014	1.165
180	0.003	−0.691	−0.119	−0.033	0.013	0.524	0.038	0.349	0.099	−0.011	1.151
200	0.064	−0.730	−0.124	−0.037	0.016	0.546	0.042	0.304	0.112	−0.008	1.091
220	−0.134	−0.768	−0.135	−0.044	0.014	0.556	0.037	0.264	0.121	−0.009	1.041
240	−0.203	−0.809	−0.144	−0.046	0.018	0.565	0.033	0.229	0.132	−0.005	1.006
260	−0.263	−0.844	−0.147	−0.047	0.021	0.574	0.033	0.196	0.148	0.000	0.940
280	−0.323	−0.876	−0.155	−0.054	0.019	0.575	0.025	0.167	0.159	0.000	0.871
300	−0.386	−0.913	−0.166	−0.059	0.019	0.570	0.014	0.141	0.169	0.001	0.823
320	−0.445	−0.950	−0.170	−0.057	0.024	0.570	0.008	0.117	0.187	0.008	0.769

the best over-all fit to the data in the energy range $E_{\text{lab}}<310$ Mev within this framework (hard core, no triplet odd-parity central force, and Yukawa-shaped potentials.)

The potential so obtained is characterized as follows:

$$^3r_0^-=0.4125,\quad ^3V_T^-=-22\text{ Mev},\quad ^3\mu_T^-=0.8,\quad ^3V_{LS}^-=7317.5\text{ Mev},\quad ^3\mu_{LS}^-=3.7. \tag{10}$$

The fits to the data obtained from the potential of Eqs. (3), (4), (9), (10) are shown in Figs. 1 and 2 (solid curves).

The fact that the best fit to the 310-Mev phase shifts required a somewhat weaker tensor force than that required by the lower energy (18.3–70 Mev) data, suggests that a change in the shape of the tensor force may result in considerable improvement of the over-all fits. To obtain a smaller effective potential at high energies than at low, a less singular potential is indicated. To test this hypothesis, calculations were performed with a tensor force having the shape:

$$V_T(r)=V_T(1-r_0/r)\exp(-\mu r)/\mu r. \tag{11}$$

This potential vanishes at the core edge. For such a tensor potential with a Yukawa-shaped spin-orbit potential, no triplet central force, and the singlet interaction as given by Eqs. (3) and (4), the triplet

interaction which best fits the data is described by the following parameters:

$$^3r_0^-=0.4125,\quad ^3V_T^-=-26\text{ Mev},\quad ^3\mu_T^-=0.8,$$
$$^3V_{LS}^-=7122.5\text{ Mev},\quad ^3\mu_{LS}^-=3.7. \tag{12}$$

An interaction of this form is negligibly different from the interaction given by Eqs. (9) and (10) at low energies, while it improves the fit to the 310-Mev phase shifts. This is illustrated in Figs. 1 and 2. The dashed curves are drawn for the potential of Eqs. (3), (4), (11), and (12) wherever this potential is significantly different from the potential of Eqs. (3), (4), (9), and (10). The polarization at 45° as a function of energy calculated from the potential of Eqs. (3), (4), (11), (12) is shown in Fig. 3, and the triplet phase shifts as a function of energy calculated from this potential are shown in Table IV and Fig. 4. The singlet phase shifts calculated from the potential Eq. (4) are shown in Fig. 5.

VII. PHASE SHIFT ANALYSIS OF THE 170- AND 310-MEV DATA

The calculated 170-, 240-, and 310-Mev angular distributions do not give a precise fit to the experimental angular distributions. This is not a serious difficulty. At 310 Mev all of the calculated phase shifts are close to the phase shifts of solution 1 of Stapp *et al.* (see Table V) and these latter phase shifts provide a precision fit to all of the experimental data at 310 Mev.

In Figs. 1 and 2, the curves drawn with alternating short and long dashes and the curves drawn with the dashes are calculated with the triplet odd-parity phase shifts calculated from the potential of Eqs. (3), (4), (11), and (12). The long-short dash curves are calculated with the singlet phase shifts of Stapp *et al.* and the dash curves with the singlet phase shifts calculated from the potential given by the singlet even-parity potential of Eqs. (3) and (4). Even this slight change in the singlet phase shifts results in a marked improvement in the shape of the 310-Mev angular distribution, and an improvement in the fit to the 310-Mev polarization data at low angles. Singlet even-parity potentials of different *shape* (different from hard core with Yukawa attraction outside) would have to be considered in order to get a better *simultaneous* fit to the singlet zero-energy scattering length and effective range and the singlet phase shifts of Stapp *et al.* at 310 Mev.

It has also been checked that at 170 Mev, small changes in the calculated phase shifts (changes similar to the difference between the calculated phase shifts at 310 Mev and the phase shifts of Stapp *et al.* for solution 1 at 310 Mev; see Table V) provide a precision fit to the experimental data, as shown in Fig. 6.

The most important differences between the phase shifts calculated from the potentials of Eqs. (9), (11), and (12) and the phase shifts of solution 1 of Stapp *et al.* occur in the $^3P_0$ and $^3F_4$ phase shifts and the

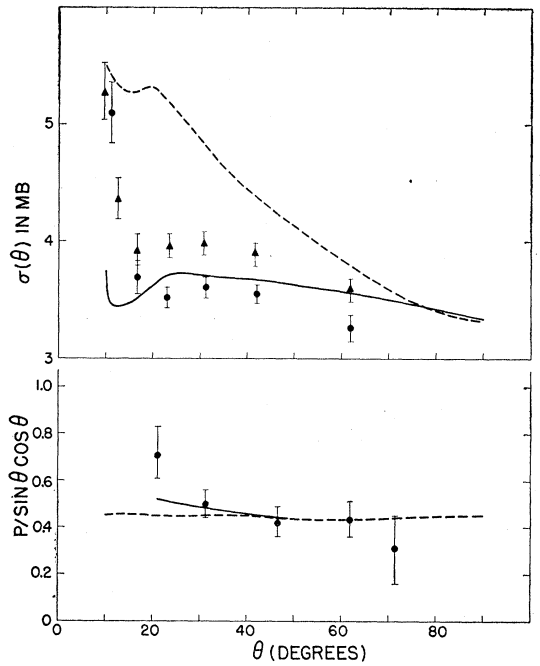

FIG. 6. The cross section and polarization at 170 Mev. The dashed curves represent the differential cross section and polarization calculated with the potentials of Eqs. (9), (11), and (12). The solid curves represent the differential cross section and polarization calculated from the adjusted phase shifts shown in Table V.

$J=4$ coupling constant. The origin of difficulties encountered in trying to better fit the phase shifts of solution 1 is that the $\mathbf{L}\cdot\mathbf{S}$ potential is not entirely negligible in the F states (see Table VI).

Investigation reveals that no further significant improvement in the fits can be obtained without allowing modifications in the shapes of the potentials. The authors plan to return to the problem of finding

TABLE V. Comparison of phase shifts calculated from potential and phase shifts obtained from phase-shift analyses.[a]

	170 Mev		310 Mev	
	Calculated from potential	Adjusted	Calculated from potential	Solution (1) of Stapp *et al.*
$\delta(^1S_0)$	0.295	0.260	−0.328	−0.353
$\delta(^1D_2)$	0.345	0.290	0.533	0.499
$\delta(^1G_4)$	0.035	0.017	0.089	0.0349
$\delta(^3P_0)$	0.0399	−0.050	−0.417	−0.499
$\delta(^3P_1)$	−0.669	−0.670	−0.932	−0.930
$\delta(^3F_3)$	−0.114	−0.100	−0.169	−0.143
$\delta(^3H_5)$	−0.033	0	−0.058	+0.003
$\delta(^3H_6)$	0.011	0.022	0.021	0.045
$\delta(^3P_2)$	0.512	0.472	0.570	0.575
$\delta(^3F_2)$	0.036	0.04	0.010	0.015
$(2\epsilon_2)$	0.373	0.373	0.128	0.125
$\delta(^3F_4)$	0.092	0.08	0.177	0.130
$\delta(^3H_4)$	−0.013	−0.013	0.004	0.030
$(2\epsilon_4)$	1.162	1.40	0.799	0.934

[a] A sign convention opposite to that of Stapp *et al.* is used for the coupling constants.

TABLE VI. Effect of spin-orbit potential in F states.

State	Phase shifts calculated from the potential of Eqs. (9), (11), and (12)	Phase shifts calculated from the same potential except that the spin-orbit term is omitted.
$^3F_3$	−0.169	−0.148
$^3F_4$	0.177	0.110
$2\epsilon_4$	0.799	1.40
$^3F_2$	0.010	0.137

the best over-all fit to the data when the potentials are allowed to have arbitrary shapes.

VIII. DISCUSSION

(A) For small distances, the nucleon-nucleon interaction must really be of the form of a (nonlocal) potential matrix $V(\mathbf{r},\mathbf{r}')$. For the energy range in which we are interested, it does not matter what the exact form of this matrix is; all that matters is the logarithmic derivative which the wave function has when it emerges from this region. Presumably this logarithmic derivative is energy-independent in the energy range (0–310 Mev) because the interaction is strong.

The spin-orbit force we find sticks right against the edge of the hard core. Its main function is to give a boundary condition which is different for the $^3P_0$, $^3P_1$, and $^3P_2$ states for at a core radius which is something like the radius of the hard core plus the range of the spin-orbit potential. For a core size $r_0=0.7$, boundary conditions $r_0u'/u=+\infty$ for the $^3P_0$ and $^3P_1$ states and $r_0u'/u=0.6$ for the $^3P_2$ state, together with a tensor potential similar to the tensor potentials found in the main work, give the same sort of ^3P phase shifts as shown in Fig. 4.

Our results may be summarized as follows: the core region ($r_0<0.7$) is much less repulsive for the $^3P_2$ state than for the $^3P_0$ and $^3P_1$ states.

(B) If the *long-range* nucleon-nucleon interaction is a consequence of the interaction of nucleons with a pseudoscalar symmetric pion field, then the *long-range* nucleon-nucleon potential should be of the form central plus tensor potentials. There should be no *long-ranged* spin-orbit potential. We make this judgment on the basis of calculations of the nucleon-nucleon potential by Brueckner and Watson,[14] Gartenhaus,[15] Lévy,[16] Taketani,[17] and others.

Thus it is very satisfying that we find a spin-orbit potential which has a *short range.* Possible origins of short-range spin-orbit force (or explicitly J-dependent force with an interval rule different from the tensor force) are interaction of nucleons with mesons of mass larger than the pi-meson mass, or perhaps nucleon recoil or some other effect not included in usual calculations of the nucleon-nucleon interaction from pi-meson theory.

(C) We have not discussed the problem of charge independence in this paper. Presumably there may be a short-range spin-orbit interaction in the triplet even-parity states which might affect the ^3D phase shifts at high energy (310-Mev). It is to be expected that such a short-range spin-orbit interaction would not be effective at low energies or in the bound state of the deuteron, because, on the one hand, $\mathbf{L}\cdot\mathbf{S}=0$ for the $^3S_1$ state and, on the other, the D states do not penetrate the core region at low energy.

We have made a preliminary fit of the 90-Mev *n-p* data using triplet even-parity potentials given in reference 1, triplet odd-parity potentials and singlet even-parity potentials given in this paper, and adjusted the singlet odd-parity interaction to fit the data. The fits have the same quality as those found in our earlier work (reference 1). In particular, the difficulty of finding calculated angular distributions which are too V-shaped remains (as might be expected since the new feature used in this work—the short-ranged triplet odd-parity spin-orbit force—is not effective at 90 Mev). Work is in progress to determine the origin of this difficulty and the possible role of a triplet even-parity short-range spin-orbit interaction in *n-p* scattering.

[14] K. A. Brueckner and K. M. Watson, Phys. Rev. **92**, 1023 (1953).
[15] Solomon Gartenhaus, Phys. Rev. **100**, 900 (1955).
[16] M. Lévy, Phys. Rev. **84**, 441 (1951); H. Gelernter, Phys. Rev. **105**, 1068 (1957).
[17] M. Taketani, Progr. Theoret. Phys. (Japan) **7**, 35 (1952).